

No Battery Required

*Sangkil Kim,
Chiara Mariotti,
Federico Alimenti,
Paolo Mezzanotte,
Apostolos Georgiadis,
Ana Collado,
Luca Roselli, and
Manos M. Tentzeris*



© PHOTOSEARCH & INGRAM PUBLISHING

Over the last decade, radio frequency identification (RFID) systems have been increasingly used for identification and object tracking due to their low-power, low-cost wireless features. In addition, the explosive demand for ubiquitous rugged low-power, compact wireless sensors for Internet-of-Things, ambient intelligence, and biomonitoring/quality-of-life application has sparked a plethora of research efforts to integrate sensors with an RFID-enabled platform. The rapid evolution of large-area electronics printing technologies (e.g., ink-jet printing and gravure printing) has enhanced the development of low-cost RFID-enabled sensors as well as accelerated their large-scale deployment. This article presents a

Sangkil Kim (ksangkil3@gatech.edu) and Manos M. Tentzeris (etentze@ece.gatech.edu) are with the School of Electrical and Computer Engineering, Georgia Institute of Technology, Atlanta, GA, 30332-250, USA. Chiara Mariotti (chiara.mariotti@studenti.unipg.it), Federico Alimenti (federico.alimenti@diei.unipg.it), Paolo Mezzanotte (paolo.mezzanotte@diei.unipg.it), and Luca Roselli (luca.roselli@diei.unipg.it) are with the Department of Electronic and Information Engineering, University of Perugia, 06125 Perugia, Italy. Apostolos Georgiadis (ageorgiadis@cttc.es) and Ana Collado (acollado@cttc.es) are with the Centre Tecnologic de Telecomunicacions de Catalunya, CTTC, Castelldefels 08860, Spain.

Digital Object Identifier 10.1109/MMM.2013.2259398
Date of publication: 11 July 2013

brief overview of the recent progress in the area of RFID-based sensor systems and especially the state-of-the-art RFID-enabled wireless sensor tags realized through the use of ink-jet printing technology.

What Is RFID?

RFID is a promising and emerging wireless technology that can be applied to thousands of applications such as tracking, finance, retail management, sports games, logistics, security, and health care, as shown in Figure 1 [1]–[3]. Its operating principle was discussed in [4], and the performance of the most recent RFID systems have rapidly improved due to the significant progress in the area of RF integrated circuits (RFICs), antenna design, and large-area printed electronics technologies, which have enabled the low-cost mass production of RFID systems [5]–[9]. An RFID system usually consists of two components: tags and readers. A reader interrogates a tag by sending an electromagnetic (EM) signal, and then the tag sends back

its unique identification information or additional data such as product information. The RFID tags are usually extremely cheap (~US\$0.10–0.20 in large quantities) and can be easily integrated with wireless sensor networks (WSNs) [10]. In addition, there are already numerous standards such as the International Organization for Standardization (ISO) and Electronic Product Code (EPC), which allow for the simultaneous interrogation of multiple tags with a low data-collision probability for a variety of environments and tag configurations [11]–[13].

There are three types of RFID tags: active, semiactive, and passive [14]–[16], with their main difference being the tag power source. The active RFID tag is fully powered by a battery and allows the tag to generate and send its identification signal by itself while the passive tag does not have any power source and uses the incident power from the reader to send back the corresponding information signal through back-scattering mechanisms. Semiactive tags use a battery

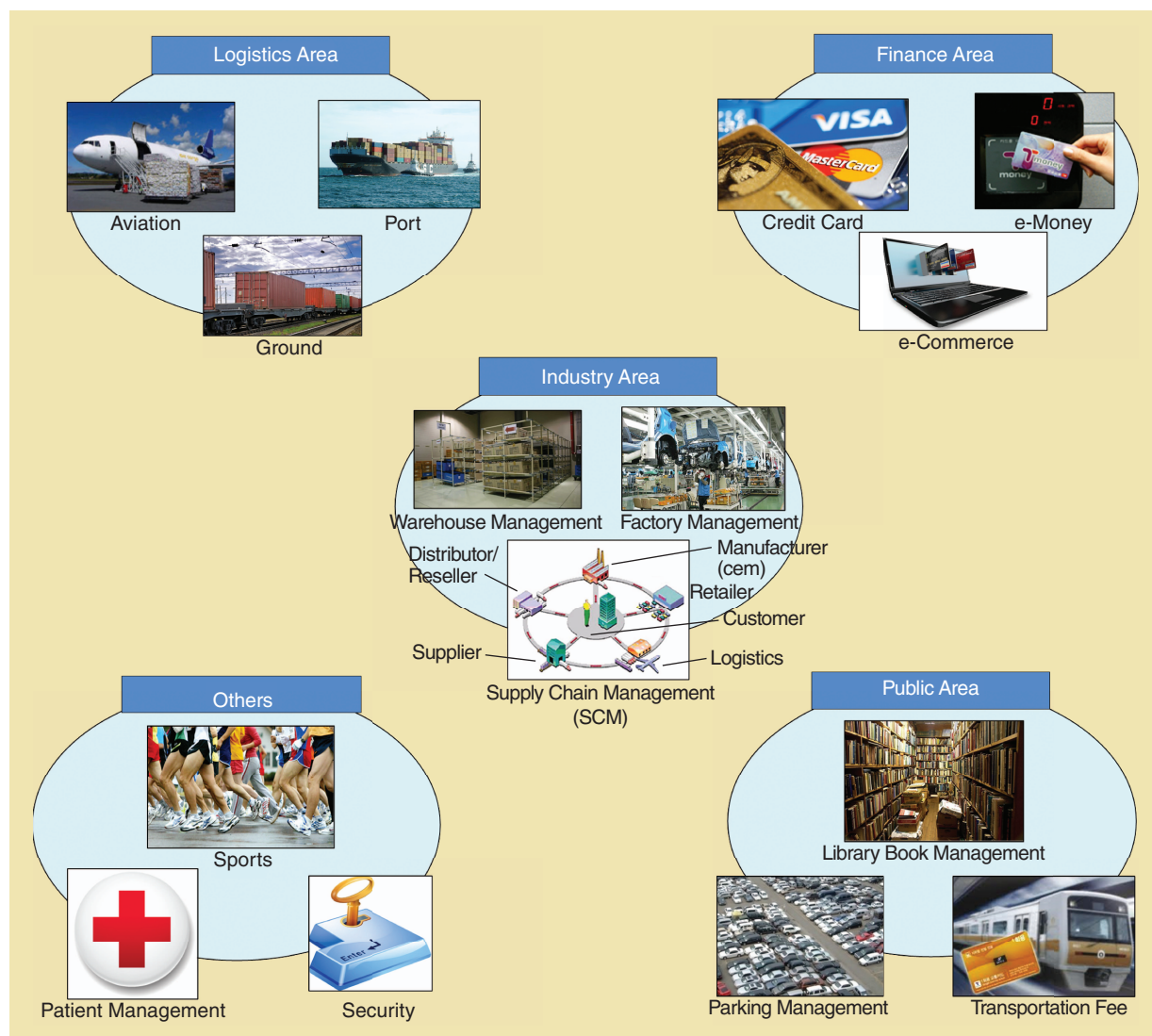


Figure 1. RFID application areas.

RFID is a promising and emerging wireless technology that can be applied to thousands of applications such as tracking, finance, retail management, sports games, logistics, security, and health care.

to activate their circuitry, but the communication is done using the backscattering mechanism. As it can be expected, the read range of passive tags is much shorter than active tags, but the active RFIDs require a battery replacement periodically. On the other hand, the price of passive tag readers is usually higher than that of active tag readers due to more demanding specifications associated with the power level required to read passive tags. The passive tags are usually used for inventory item-level identification whereas the active tags are used for real-time item-status sensing and tracking or monitoring.

From RFID to RFID-Enabled Wireless Sensor

RFID systems have a lot of attractive advantages and great potential as low-power wireless platform for sensing applications. First of all, the cost of RFID tags is typically very low and could be further reduced by employing cost-efficient fabrication technologies, such as ink-jet printing technology on low cost substrate such as paper or plastics [17]–[20]. Implementing a low cost RFID-enabled sensor tag is very crucial for the realization of the first Internet-of-Things configurations and cognitive intelligence applications requiring

large amounts of tetherless sensor nodes. The RFID systems have a simple architecture which consists of tags and readers whereas the conventional WSNs consists of sensor/relay nodes with numerous electronic components and mixed-signal interfaces. Recently, it was demonstrated that RFID systems can be made compatible with conventional WSN [21]. Additionally passive RFID tags not only have a longer life time than other active sensor devices but also have lower consumption [22]. Moreover, over the last five years there have been many preliminary demonstrations of RFID-enabled sensors in various domains, such as temperature [23], gas [24], [25], strain [26], water quality [27] and humidity [28] monitoring.

Most RFID-enabled sensors are integrated with selected sensing materials depending on the sensing target such as water absorbing materials for humidity sensor or carbon nanostructures for gas sensors. The chemical, physical, or electrical reaction of the sensing materials in the presence of the sensed parameters modify their electrical properties (permittivity, conductivity) resulting in easy-to-observe electrical metrics, such as a shift of the resonant frequency of the RFID tag antenna as shown in Figure 2, verifying the simplicity and power efficiency of RFID-enabled sensors [29]. In this article, a variety of ink-jet-printed RFID-enabled sensor prototypes are briefly discussed and perpetual RFID-enabled sensing platforms for cognitive intelligence applications are introduced.

Ink-Jet Printing Technology

Ink-Jet Printing of Nanoparticle Ink

Over the last decade, there have been dramatic advances in the area of large-area electronics' printing technologies that have enabled the realization of printed electronics on various substrates including flexible and organic substrates. The development of nanoparticle inks made of various materials such as metals, carbon based nanostructures, polymers, and semiconducting materials [25], [30]–[35] have further enhanced the capabilities especially of ink-jet-printed fabrication process that are typically cheap, efficient, and environmentally friendly due to their additive character in contrast to other widely used fabrication methods, such as etching which is a subtractive fabrication method. Additive processes like ink-jet printing technology deposit nanoparticle conductor ink drops on the exact desired position, while subtractive processes remove unwanted metallization areas from the surface of substrates utilizing acids and heavy chemicals [36]. Ink-jet printing technologies also enable the rapid fabrication of any shape of patterns with resolutions down to 15 μm eliminating the need of any wet processes, such as photolithography; there have recent reports of an even better printing resolution down to the submicron range [37].

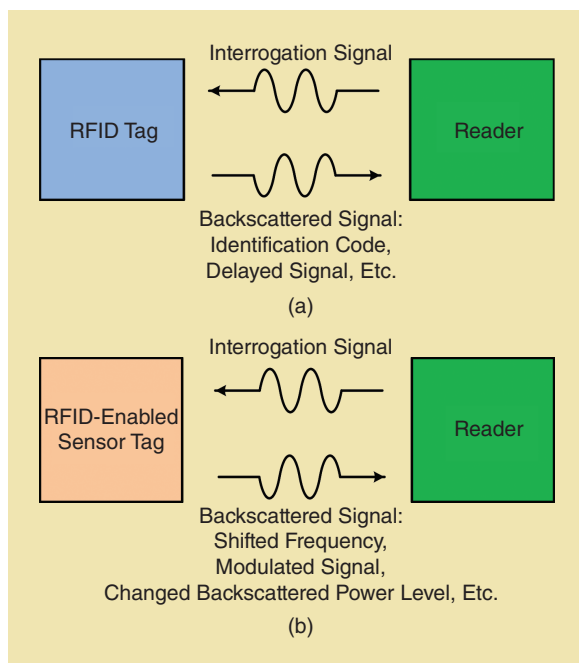


Figure 2. (a) RFID tag and (b) RFID-enabled sensor tag.

The mean diameters of the drops of the silver nanoparticles are about $28 \mu\text{m}$ with droplet volumes of 1 pL and 10 pL respectively [38]. It is important to select and optimize proper ink droplet volume, drop spacing between ink droplets, waveform for the ink-jet nozzle, nozzle temperature, and temperature of the substrate for the optimal printing resolution, accuracy and repeatability.

Properties of Ink-Jet-Printed Nanoparticles

Especially, silver nanoparticle inks have been widely used and investigated among many types of nanoparticle inks made from silver (Ag), copper (Cu), and gold (Au) due to their low sintering temperature and high conductivity properties. Silver nanoparticles form an agglomeration of silver particles once they are printed, and each particle is surrounded by a polymer coating that helps nanoparticles keep in the form of ink. It has to be stressed that a sintering process through the use of laser, ultraviolet flash lamp, or microwave heating [40]–[42] is required to make the printed ink sufficiently conductive by burning off the polymer coating and the solvent impurities. Additionally, the sintering process melts the particles together and increases the bond of the silver trace with the substrate. The critical factors that affect significantly the conductivity of the printed traces include the number of printed layers, the surface roughness of the substrate, the sintering temperature, and the nanoparticle concentration of the ink. Figure 3 shows the scanning electron microscope (SEM) image before/after sintering process at the 150°C for 15 min. The silver nanoparticle agglomerations [Figure 3(a)] as well as the formation of a conductive metal sheet [Figure 3(b)] can be clearly observed. Figure 4 shows the image of the printed silver nanoparticle surface using Veeco atomic force microscopy (AFM) [39]. The measured arithmetic average (R_a) and root mean squared (R_q) roughness is 11.4 nm and 14.4 nm, respectively verifying the applicability technologies up to millimeter-wave applications.

The mechanical and electrical properties of ink-jet-printed silver nanoparticles have been reported in previous works [43]–[44]. The Young modulus of the thermally sintered silver trace is a function of sintering temperature and pull-off breaking force of the printed silver traces is about 50 N. The quantity of water in a substrate mainly affects the adhesion strength of the printed traces to the substrate rather than the conductivity of the printed conductors [44]. The electrical properties of the ink-jet-printed silver nanoparticle inks are reported in [38] and [43]. The printed patterns using a 10 pL cartridge of ink with $20\text{-}\mu\text{m}$ drop spacing (1024 dpi) have been sintered in a thermal oven at atmospheric pressure, and the sheet resistance of the traces is measured using Cascade’s four-point probe station with values shown in Figure 5(a) for different numbers of printed layers and at different sintering

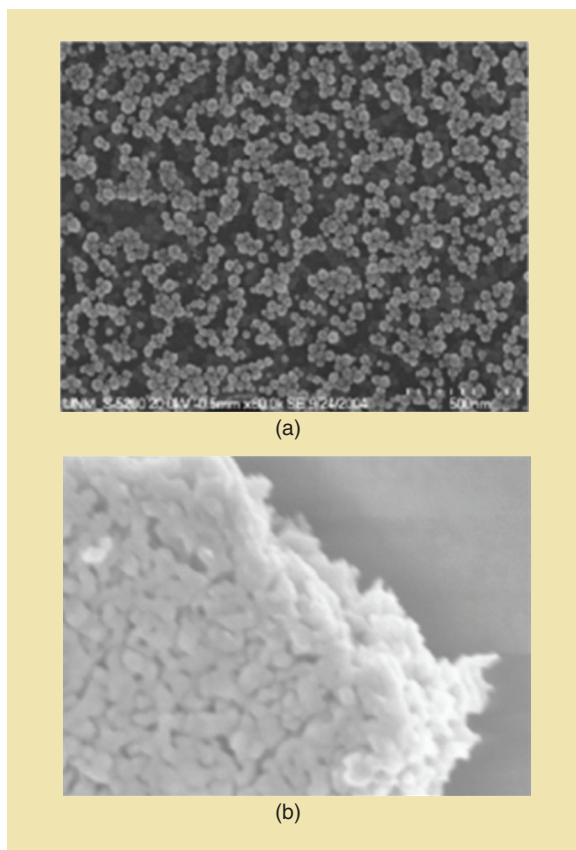


Figure 3. SEM image of ink-jet-printed silver nanoparticles (a) before sintering (particle size $\sim 30 \text{ nm}$) and (b) after sintering at 150°C for 15 min [27].

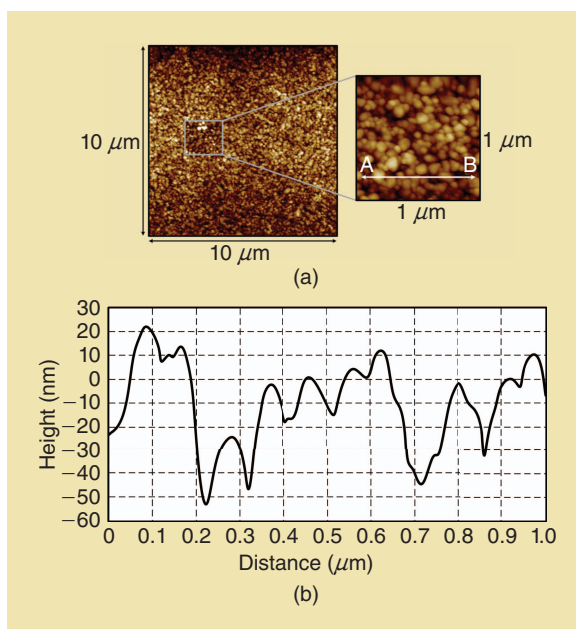


Figure 4. (a) The surface of the ink-jet-printed silver nanoparticle inks. (b) Cross section of the line AB [36].

temperatures. It is obvious that the sheet resistance decreases as sintering temperature and number of printed layers increases due to the fact that the higher temperature burns off a larger amount of the polymers

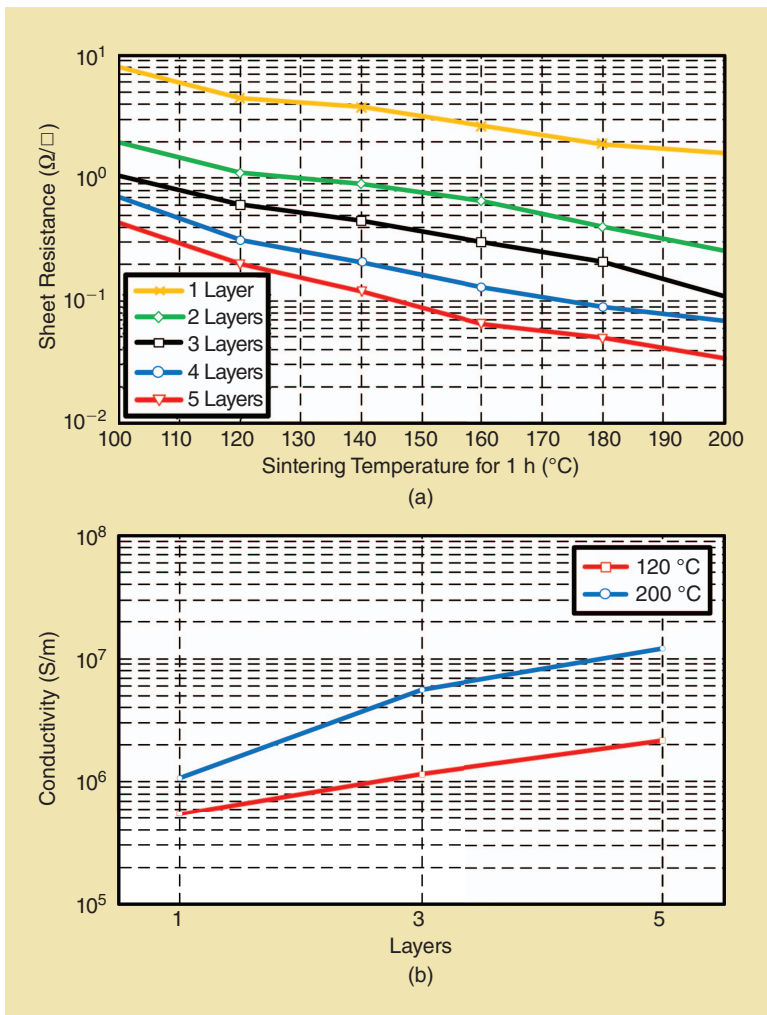


Figure 5. (a) Sheet resistance versus sintering temperature and (b) extracted conductivity of the printed silver traces versus number of printed layers [35].

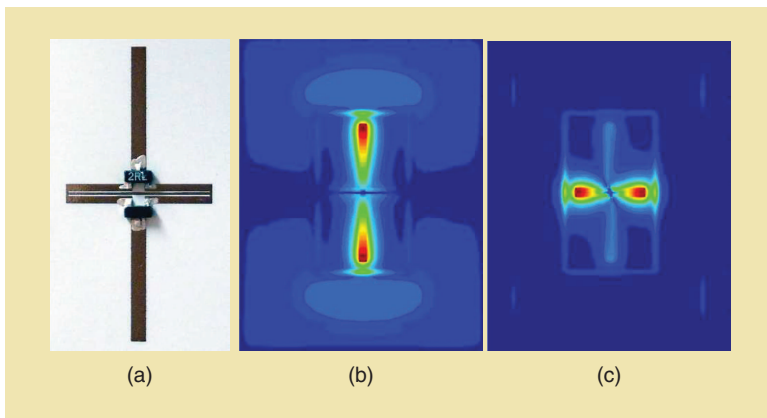


Figure 6. One-bit harmonic tag based on crossed dipoles and Schottky diodes frequency doubler. (a) Prototype on paper substrate, (b) E-field distribution of the received field at $f_0 = 3.5$ GHz, and (c) of the irradiated field at $2f_0 = 7$ GHz [43]. (Reprinted from [32].)

coatings and helps to form a good percolation channel for electron flow, while adding more layers increases the particle density, thus resulting in more uniform and solid structure. The thickness of the layers was

measured to extract the conductivity values from the sheet resistance using a Dekktak profilometer. The printing of each individual layer adds approximately 250 nm and 500 nm of metalization thickness for 1 pL and 10 pL cartridges, respectively. The conductivity can be extracted using the cross-section area of the printed trace and the sheet resistance as its value is inversely proportional to their product. The extracted conductivities are shown in Figure 5(b). The maximum value of the conductivity is 1.2×10^7 S/m, which is about 18.75% the one of bulk silver (6.4×10^7 S/m) and is very similar to the conductivity of bulk iron (1.04×10^7). It has to be stressed that a very recent paper [45] reported for the first time the electroless and nonoxidized deposition of copper over the large surface of paper substrate-though the ink-jet printing of an appropriate catalyst with similar performance to the ink-jet-printed silver nanoparticle inks for a drastically reduced cost and a much more environmentally friendly (green) configuration. Also, [46] reported the first flexible multilayer ink-jet-printed capacitors with a self resonant frequency above 3 GHz utilizing two custom formulated polymer-based dielectric inks (SU8 and PVP) with quality factor from 4 ~ 8. As a conclusion, the ink-jet printing of nanoparticles-based inks can be effectively used for the implementation of low-cost flexible microwave devices, such as RFIDs and sensors.

Passive, Chipless, Harmonic RFID-Based Sensor

The first ink-jet-printed RFID prototype that is presented in this article relies on the principle of harmonic RFIDs. A harmonic tag is a circuit that, when interrogated at a frequency f_0 , retransmits an answer at a harmonic frequency $n \cdot f_0$. Since a frequency multiplier can be realized exploiting the nonlinearity of a varactor or of a Schottky diode, harmonic tags are typically passive circuits. The advantage of this idea is that the tag response is generated at a

perfectly known frequency, thus the presence or the absence of such a signal can easily be determined. Similar techniques have been used in harmonic radar systems [47].

An example of a passive, one-bit, RFID harmonic tag is constituted by the structure shown in Figure 6 [48]. It consists of two crossed $\lambda/2$ -dipoles. The longest dipole receives the incoming power at the fundamental frequency f_0 , whereas the shortest dipole transmits the generated power at the doubled frequency $2f_0$ in an orthogonally polarized orientation, [49]. Such a principle is apparent from the lumped-element finite difference time domain (LE-FDTD) simulations reported in Figure 6(b) and (c).

The frequency multiplication is achieved by four diodes in a bridge configuration, thus forming a fully balanced multiplier bridge. Although the diodes are operating self-biased and no external dc-supply is necessary, a return for the generated dc-component must be provided for the proper operation of the frequency multiplier itself. This is done with a thin metal strip that is embedded in the short dipole connecting its outer ends. Thus a sufficient amount of inductance is provided to avoid a significant perturbation of the RF performances.

To further develop the harmonic tag concept, however, one must be able to use it for the transmission of sensor data.

Exploiting Orthogonal Antennas

A first possibility to transmit sensor data by means of a harmonic tag has recently been published in [50] and uses the tag circuit of Figure 7. The basic idea is to encode the sensor information as the phase difference between two signals transmitted by two orthogonal antennas, one acting as the reference for the other one. In this way an accurate, relative measurement is possible.

To describe the tag operation let's consider the signal flow shown in the Figure 7. The incoming EM wave at frequency f_0 is received by a spiral or an helical antenna. In this way the power at the antenna output is maximized regardless of the polarization or the relative reader-tag orientation. The received power is then fed into a varactor or a Schottky diode frequency doubler, and the second harmonic is generated. At this point the $2f_0$ signal is split by a power divider. The first part is directly reradiated in vertical polarization (e.g., E_η in Figure 7) in such a way as to form a reference signal component. The second part, instead, is phase-shifted by the angle, $\Delta\phi$, and then reradiated in horizontal polarization (e.g., E_ξ in Figure 7).

The phase angle ($\Delta\phi$) encodes the sensor information and must be recovered by the reader. To this purpose the reader is composed of four subsystems, as depicted in Figure 8. A phase-locked loop (PLL) oscillator is used to generate both the f_0 and the $2f_0$ signals in a synchronous way. Then, two I/Q receivers are used to retrieve the phase information.

Exploiting Impedance Bridges

The second way to transmit sensor data using harmonic tags is shown in Figure 8. It is composed by a receiving

RFID systems have a lot of attractive advantages and great potential as low-power wireless platform for sensing applications.

antenna at $f_0 = 868$ MHz, a Schottky-diode frequency multiplier that generates the second harmonic $2f_0$, an impedance bridge and an antenna transmitting the processed second harmonic signal.

The impedance bridge has a key role in the sensing operation. The variable impedance Z_g is realized with a carbon nanotube (CNT) deposition suitably dimensioned to be close (ideally equal) to the other impedances (Z) of the bridge. With this approach, when no gas is present, the output voltage of the bridge is zero and there is no signal at $2f_0$ transmitted by the tag. As a result, the

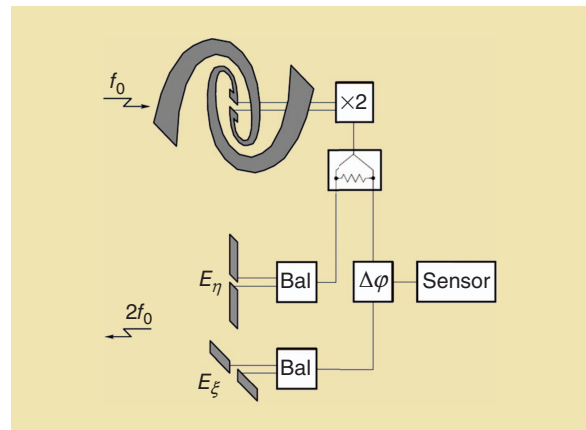


Figure 7. Harmonic tag block diagram for the system with two orthogonal antennas. The sensed quantity alters the phase of one channel, with the other being used as a reference one [50].

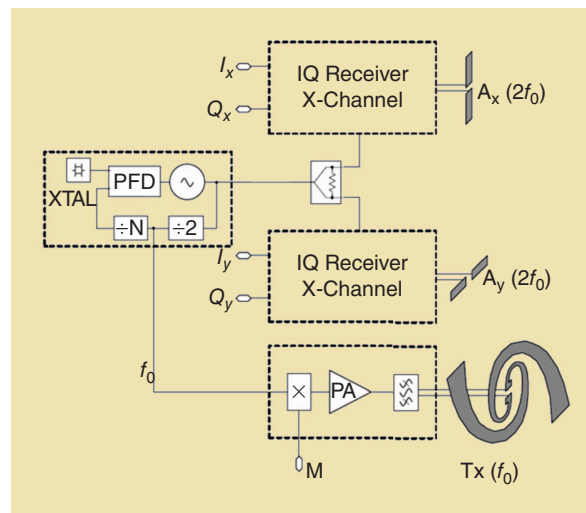


Figure 8. Block diagram of a passive RFID tag sensor exploiting harmonic generation and impedance bridge concepts [50]. (Reprinted from [32].)

It is worth underlining that the proposed architecture is chipless, i.e., does not require complex chips, thus it is inherently low cost and quite attractive for mass production and WAEs.

zero level (no gas present) of the final measurement is well referred to impedance standards instead of being determined by the matching between CNT layer and antenna, as in [51].

The gas detection by the reader needs hence two conditions to be verified simultaneously:

- the presence of the harmonic tag (significant to underline the false alarm robustness due the harmonic tag)
- the unbalance of the bridge, that is verified when the gas presence modifies the CNT impedance, Z_g .

With such an approach the signal modulation is provided, at tag level, directly by Z_g , whereas the harmonic operation results in a strong immunity to backscattering and interferences from the surrounding environment.

It is worth underlining that the proposed architecture is chipless, i.e., does not require complex chips, thus it is inherently low cost and quite attractive for

mass production and wide-area electronics (WAEs). This is even more important in the future vision of ink-jet or screen printing fabrication approaches on recyclable materials.

Referring to the impedance bridge in Figure 9, the voltage measured at the bridge output terminals, V_o , is given by

$$V_o = \frac{Z_a}{Z + Z_a} \left(\frac{Z}{Z + Z_g} - \frac{1}{2} \right) V_{2nd}, \quad (1)$$

where V_{2nd} is the second harmonic voltage feeding the impedance bridge and Z_a is the input impedance of the antenna reirradiating the signal at $2f_0$. Considering that

$$Z_g = Z + \Delta Z_g, \quad (2)$$

i.e., that without gas the bridge is in equilibrium, the output voltage (V_o) can be rewritten as

$$V_o = \frac{Z_a}{Z + Z_a} \left(\frac{Z}{2Z + \Delta Z_g} - \frac{1}{2} \right) V_{2nd}. \quad (3)$$

As a consequence, for small variations of the CNT impedance, ΔZ_g is small and the output voltage is approximated by

$$V_o \approx -\frac{Z_a}{Z + Z_a} \frac{\Delta Z_g}{4Z} V_{2nd}. \quad (4)$$

It is important to observe that, with respect to previous pioneering implementations of the CNT gas sensor, in the present architecture the quiescent condition corresponds to a zero signal emitted from the tag. This means that the sensitivity of the system, and thus its dynamic range, depends primarily on the balance among the three reference resistors and that constituted by the CNT layer, in the absence of gas.

A proof-of-concept of the above described sensor can easily be done exploiting a circuit simulator with harmonic-balance (HB) capability. In particular, we have implemented the circuit schematic shown in Figure 10. In Figure 10, C models the parasitic capacitance due to the metal traces contacting the CNT deposition. This capacitance has also been added to the other impedances in order to improve the bridge equilibrium in the absence of gas. The equivalent CNT circuit model with and without NH_3 is shown in Table 1 [52]. These values have been obtained fitting the experiments reported in [29], with a simple model constituted by a resistor R_g in parallel with a capacitance C_g .

At this stage, two CNTs are placed in the two opposite arms of the bridge in order to double the output voltage

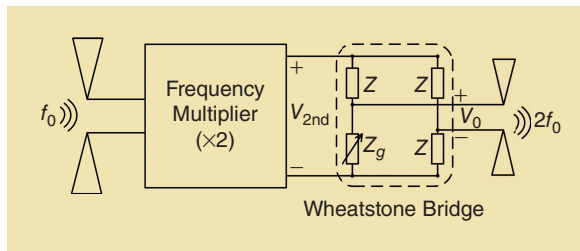


Figure 9. Block diagram of a passive RFID tag sensor exploiting harmonic generation and impedance bridge concepts. (Reprinted from [51].)

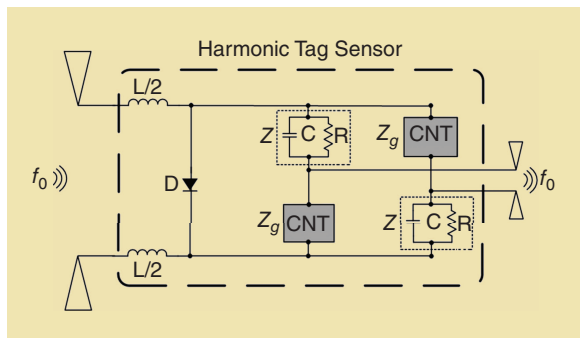


Figure 10. Schematic of the simulated tag circuitry. In this drawing, D is the HSMS 270C Schottky diode from HP, $L = 6.5$ nH is used for impedance matching, $R = 51 \Omega$ is the reference impedance, whereas $C = 0.4$ pF compensates for the parasitic capacitance of the CNT layer; $Z_a = 50 \Omega$ is the impedance of both antennas at f_0 and $2f_0$. The fundamental operating frequency is $f_0 = 868$ MHz [53].

TABLE 1. Equivalent CNT model at 1.7 GHz [52].

State	R_g (Ω)	C_g (pF)
No gas	51.6	0.4
4% NH_3	97.1	0.4

shown in (3). In this way, however, a layout where the CNTs are one in proximity of the other is recommended; moreover, the sensing elements have to be fabricated in order to be as similar as possible to each other.

To make the second harmonic possible, a low barrier Schottky diode (type HSMS 270C produced by Avago Technologies) is considered. In the schematic the inductance L is used to optimize the power transfer in the input section, i.e., between the antenna at f_0 and the frequency doubler.

As long as the CNT impedances is not exposed to NH_3 , the impedances of the four branches are virtually equal to each other and the bridge results balanced. This condition causes the output voltage to be zero, so that the tag will not react to a query from the reader (no alarm). As the concentration of the ammonia increases, the impedance of the CNT elements varies, unbalancing the bridge and enabling the sensor tag to respond to the reader with a $2f_0$ alarm signal.

Figure 11 shows the second-harmonic power at the tag output (i.e., delivered to the antenna) versus the available power illuminating the tag itself (at the fundamental frequency). The blue curve is the case without gas (less than 100 ppm_v of ammonia). In this situation the bridge is almost in equilibrium, with the residual unbalance being mostly due to the commercial values selected for the reference bridge resistances ($R = 51 \Omega$ in the present study). The red curve, instead, is the case when the two CNT sensing layers are under an ammonia flow. In this situation $R_g = 97$, and an alarm signal is generated. Finally, the purple curve represents the limit situation when R_g approaches infinity.

A dynamic range of about 50 dB can thus be predicted in the considered case of study that represents a great improvement with respect to the present state of the art. Furthermore, a dose of roughly 200 ppm is already able to set the alarm on.

Finally, in order to gain a deeper insight into the potential performances of the proposed sensor, the CNT resistance should be expressed in terms of the ammonia concentration. According to [29] and [54] the following model can be derived:

$$R_g \approx R_0 \frac{l}{w} (1 + \alpha \cdot c) \quad (5)$$

where c is the ammonia concentration in ppm⁻¹, R_0 is the relative sensitivity of the

CNT layer expressed in ppm⁻¹, R_0 is the sheet resistance and l/w is the aspect ratio of the deposition. In the present case the sheet resistance multiplied the aspect ratio is equal to 51.6Ω , whereas $\alpha \approx 22 \times 10^{-6}$ ppm⁻¹. From [54] one can also estimate that, for an ink-jet deposition of 25 CNT layers, the sheet resistance is $R_0 \approx 145 \Omega$.

Retrodirective Transponders for Identification and Sensing

Retrodirective antenna arrays are capable of retransmitting an interrogating signal back to its source without

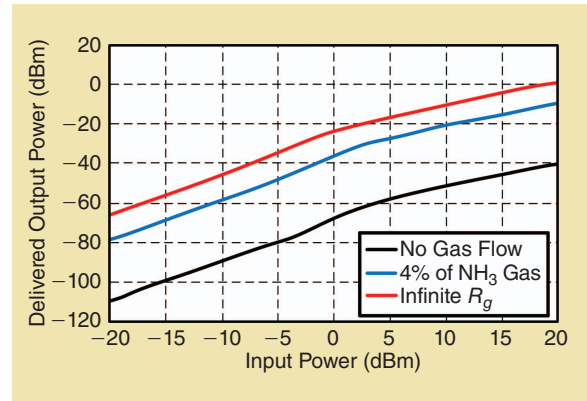


Figure 11. Second harmonic output power (delivered to the antenna) versus available input power. Legend: no gas (black), under ammonia flow (blue), and R_g approaching infinity (red). In the absence of gas the residual unbalance is due to the difference of $R_g = 51.6$ with respect to the reference resistances ($R = 51 \Omega$ corresponding to a commercial value). When the CNT sensing layers are exposed to the ammonia flow $R_g = 97.1 \Omega$.

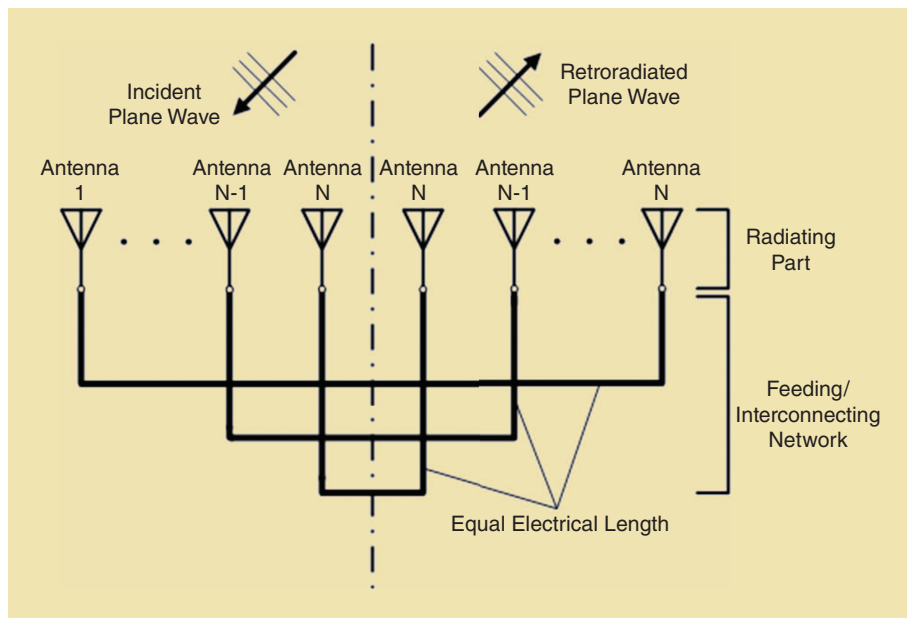


Figure 12. The concept of retrodirective Van Atta array. It consists of a linear reflector array interconnected by equal electrical lengths transmission line. The incident wave travel through the interconnecting network and are reradiated. The retroradiated wave has the reverse phase of the incident waves [57].

Over the last decade, there have been dramatic advances in the area of large-area electronics' printing technologies that have enabled the realization of printed electronics on various substrates including flexible and organic substrates.

requiring complicated circuitry and digital signal processing to compute the angle of arrival of the incoming signal [55]. As a result they are particularly suitable in applications where low cost and low complexity is important. Retrodirective performance is achieved by utilizing circuit and array topologies to perform the required phase conjugation necessary for the incoming beam to be transmitted back toward its origin. There are two main circuit topologies used to achieve retrodirective performance. In the Van Atta topology [56], pairs of antennas having the same distance from the geometrical center of the array are connected with each other with networks of equal electrical length, as shown in Figure 12 [57]. Van Atta arrays can be purely passive or

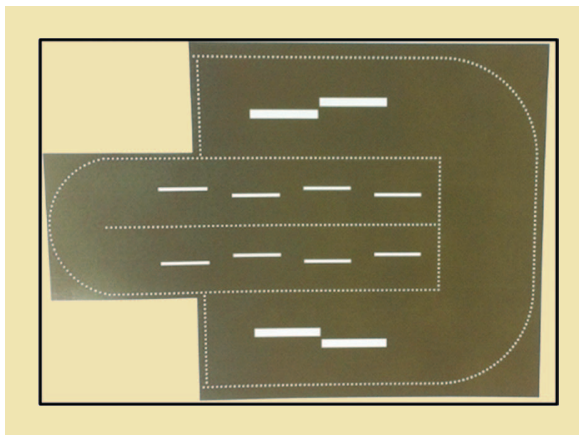


Figure 13. Photo of ink-jet-printed dual-band SIW retrodirective array on paper [67].

they may include amplifiers within the antenna element interconnecting paths in order to increase the system operating range. Active circuits are also employed in the heterodyne mixing retrodirective topology [58] where the incoming RF signal is mixed with a local oscillator having a frequency equal to twice the RF signal frequency. The self-steering capability of such systems leads to a robust system performance over a wide range of relative orientation scenarios between the interrogating source and the transponder. As a result the potential of retrodirective systems in identification and back-scatter communication applications has been quickly recognized and examples have been proposed in [59] and [60]. Recently, a bistatic RFID system based on retrodirective transponders has also been proposed [61].

Passive Van Atta retrodirective transponders are particularly attractive in cases where low power operation is required. Thus, such systems have been proposed for rectennas and rectenna arrays in order to optimize the rectified power by making the rectennas insensitive to orientation with respect to the wireless power transmitting source [61]–[63]. The possibility of robust wireless power transfer has an immediate application in powering passive RFID tags. In [64], a two element Van-Atta antenna array was used to power a commercial RFID chip demonstrating an improved angular reading range.

Passive RFID tag antenna sensors [65] as well as chipless RFID sensors [66] operate based on the principle that the radar cross section or back-scattered signal from the sensor varies depending on a desired sensing parameter. Similarly, one desires that their operation is insensitive to the relative orientation between the sensor and the reader. Retrodirective antenna sensors provide an attractive solution for such systems, especially when combined with low cost fabrication methods and flexible substrate materials. In [67], a dual band passive retrodirective array ink-jet printed on a paper substrate has been demonstrated, utilizing substrate integrated waveguide (SIW) technology, and demonstrating the potential for chipless RFID sensing applications at two different frequencies (Figure 13).

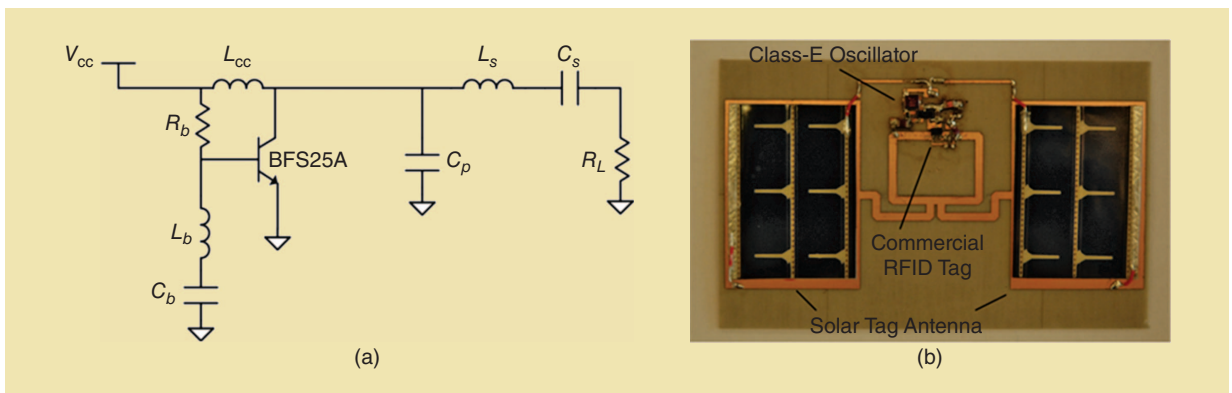


Figure 14. RFID tag with solar antenna and oscillator: (a) schematic and (b) fabricated tag [79].

Retrodirective antenna technology is more suitable in higher frequency applications due to the possibility of implementing larger and compact antenna arrays, and SIW technology further allows for low cost, low profile, and high performance circuits that do not suffer from undesired feed EM radiation at the junction discontinuities occurring when using microstrip or coplanar waveguide structures [68].

Energy Harvesting Assisted RFID

The operating range of passive RFID systems is limited by the requirement that the reader signal must provide sufficient energy to power the tag circuitry. Energy harvesting can be used to provide alternative power sources distinct from the reader signal and power the tag circuitry, thus extending the tag operating range maintaining a perpetual operability in virtually any propagation scenario. Ambient light and thermal, mechanical, and EM energy can be harvested depending on the application scenario [69].

Toward this objective, solar antennas and solar-EM harvesters provide an attractive option for compact tags as both the antenna and solar cell can be carefully designed to share the same substrate area. Solar antennas have been initially proposed for satellite applications [70]; however, the recent interest in compact sensors with energy harvesting capability has led to the design of compact solar antennas [70]–[72] for autonomous battery-less sensor operation. In addition conformal solar antennas, solar rectennas, and solar-powered sensors implemented in low cost textile [73], polyethylene terephthalate (PET) [74], [75], and paper [76] substrates using thin film amorphous silicon (a-Si) solar cells have appeared in the literature.

Solar power enhanced RFID tags were proposed in [77], and a passive RFID system operation using the wireless identification and sensing platform (WISP) and a-Si solar cells was additionally demonstrated. The dc electrical power generated by solar cells can be used as an auxiliary power source for commercial RFID tag chips, provided they allow for an auxiliary dc supply pin [79]–[78]. Alternatively, dc electrical power generated from any type of energy harvesting transducer can be first converted to RF power and then supplied into the RF input pin of a standard commercial RFID tag chip [79]. The input rectifier section of an RFID chip can efficiently convert an input RF signal within a wide frequency bandwidth to dc power, with the help of a suitable matching network. Such matching networks can be printed on the tag substrate together with the antenna. The challenge then becomes that of efficiency converting the harvested dc power into a suitable RF signal.

The concept of solar-to-microwave power transmission is not new and has been considered in solar power satellite systems, designed to collect solar power in space, convert it in microwave power, and subsequently

In order to gain a deeper insight into the potential performances of the proposed sensor, the CNT resistance should be expressed in terms of the ammonia concentration.

transmit it to earth, where rectenna systems are able to convert it back to dc electrical power [80], [81]. Space solar power has led to significant advances in microwave wireless power transmission technology, spurring research efforts in terms of high power and efficient microwave sources, power amplifiers, active antennas, and rectennas [81]–[82]. The same principle can be applied into powering low-profile, low-power RFIDs and sensors. As a result, low-power but highly efficient dc-RF converter circuits such as class-E oscillators and active antennas operating in UHF frequencies are considered [83]. An example of an RFID tag additionally powered using a solar active antenna oscillator is shown in Figure 14 [79].

Summary

This article has introduced the concept and design examples of perpetual RFID-enabled wireless sensors for cognitive intelligence applications taking advantage of the low-cost, recently developed ink-jet-printing technologies. The concept is verified by the enhanced dynamic range of an ink-jet-printed passive harmonic sensor tag utilizing the Wheatstone bridge. Ink-jet-printed, retrodirective transponders for identification and sensing as well as a standalone RFID tags integrated with a solar panel that combines the concept of solar antennas and solar-EM harvesters, further stress the potential of the proposed approach for the fabrication of low-cost, low-power autonomous flexible RFID-enabled sensing modules on virtually every low-cost substrate up to the millimeter-wave frequency range.

Acknowledgment

The work of A. Georgiadis and A. Collado was supported by EU Marie Curie FP7-PEOPLE-2009-IAPP 251557 and by the Spanish Ministry of Economy and Competitiveness project TEC 2012-39143. The work of S. Kim, and M.M. Tentzeris was supported by NSF, NEDO, and IFC/SRC

References

- [1] K. V. S. Rao, P. V. Nikitin, and S. F. Lam, "Antenna design for UHF RFID tags: A review and a practical application," *IEEE Trans. Antennas Propag.*, vol. 53, no. 12, pp. 3870–3876, Dec. 2005.
- [2] E. W. T. Ngai, K. K. L. Moon, F. J. Riggins, and C. Y. Yi, "RFID research: An academic literature review (1995–2005) and future research directions," *Int. J. Prod. Econ.*, vol. 112, no. 2, pp. 510–520, Apr. 2008.
- [3] C. Chao, J. Yang, and W. Jen, "Determining technology trends and forecasts of RFID by a historical review and bibliometric analysis from 1991 to 2005," *Technovation*, vol. 27, no. 5, pp. 268–279, May. 2007.

- [4] H. Stockman, "Communication by means of reflected power," *Proc. IRE*, vol. 36, no. 10, pp. 1196–1204, Oct. 1948.
- [5] L. Bognione, "RFID technology—Are you ready for it?," *IEEE Microwave Mag.*, vol. 8, no. 6, pp. 30–32, Dec. 2007.
- [6] S. Preradovic, N. Karmakar, and I. Balbin, "RFID transponders," *IEEE Microwave Mag.*, vol. 9, no. 5, pp. 90–103, Oct. 2008.
- [7] A. Ricci, M. Grisanti, I. De Munari, and P. Ciampolini, "Improved pervasive sensing with RFID: An ultra-low power baseband processor for UHF Tags," *IEEE Trans. Very Large Scale Integr. Syst.*, vol. 17, no. 12, pp. 1719–1729, Dec. 2009.
- [8] E. Perret, S. Tedjini, and R. S. Nair, "Design of antennas for UHF RFID tags," *Proc. IEEE*, vol. 100, no. 7, pp. 2330–2340, July 2012.
- [9] M. Singh, H. M. Haverinen, P. Dhagat, and G. E. Jabbour, "Inkjet printing—Process and its applications," *Adv. Mater.*, vol. 22, no. 6, pp. 673–685, Feb. 2010.
- [10] R. Glidden, C. Bockorick, S. Cooper, C. Diorio, D. Dressler, V. Gutnik, C. Hagen, D. Hara, T. Hass, T. Humes, J. Hyde, R. Oliver, O. Onen, A. Pesavento, K. Sundstrom, and M. Thomas, "Design of ultra-low-cost UHF RFID tags for supply chain applications," *IEEE Commun. Mag.*, vol. 42, no. 8, pp. 140–151, Aug. 2004.
- [11] International Organization for Standardization. [Online]. Available: <http://www.iso.org>
- [12] EPCglobal. [Online]. Available: <http://www.epcglobalinc.org>
- [13] ETSI—European Telecommunications Standards Institute. [Online]. Available: <http://www.etsi.org>
- [14] V. Chawla and D. S. Ha, "An overview of passive RFID," *IEEE Commun. Mag.*, vol. 45, no. 9, pp. 11–17, Sept. 2007.
- [15] R. Tesoriero, J. Gallud, M. Lozano, and V. Penichet, "Using active and passive RFID technology to support indoor location-aware systems," *IEEE Trans. Consumer Electron.*, vol. 54, no. 2, pp. 578–583, May 2008.
- [16] R. Weinstein, "RFID: A technical overview and its application to the enterprise," *IT Prof.*, vol. 7, no. 3, pp. 27–33, May–June 2005.
- [17] L. Yang, A. Rida, R. Vyas, and M. M. Tentzeris, "RFID tag and RF structures on paper substrates using inkjet-printing technology," *IEEE Trans. Microwave Theory Tech.*, vol. 55, no. 12, pt. 2, pp. 2894–2901, Dec. 2007.
- [18] V. Lakafosis, A. Rida, R. Vyas, Y. Li, S. Nikolaou, and M. M. Tentzeris, "Progress towards the first wireless sensor networks consisting of inkjet-printed, paper-based RFID-enabled sensor tags," *Proc. IEEE*, vol. 98, no. 9, pp. 1601–1609, Sept. 2010.
- [19] D. Bechevet, T.-P. Vuong, and S. Tedjini, "Design and measurements of antennas for RFID, made by conductive ink on plastics," in *Proc. IEEE Antennas Propagation Society Int. Symp.*, July 2005, vol. 2B, pp. 345–348.
- [20] S. Moles, D. R. Redinger, D. C. Huang, and V. Subramanian, "High-quality ink-jet-printed multilevel interconnects and inductive components on plastic for ultra-low-cost RFID applications," in *Proc. MRS*, 2003, vol. 769, p. H8.3.
- [21] H. Liu, M. Bolic, A. Nayak, and I. Stojmenovic, "Taxonomy and challenges of the integration of RFID and wireless sensor networks," *IEEE Network*, vol. 22, no. 6, pp. 26–35, 2008.
- [22] R. Want, "An introduction to RFID technology," *IEEE Pervasive Comput.*, vol. 5, no. 1, pp. 25–33, 2006.
- [23] D. Girbau, A. Ramos, A. Lazaro, S. Rima, and R. Villarino, "Passive wireless temperature sensor based on time-coded UWB chipless RFID tags," *IEEE Trans. Microwave Theory Tech.*, vol. 60, no. 11, pp. 3623–3632, Nov. 2012.
- [24] R. A. Potyrailo, C. Surman, S. Go, Y. Lee, T. Sivavec, and W. G. Morris, "Development of radio-frequency identification sensors based on organic electronic sensing materials for selective detection of toxic vapors," *J. Appl. Phys.*, vol. 106, no. 12, pp. 124902–124902-6, 2009.
- [25] L. Yang, R. Zhang, D. Staiculescu, C. P. Wong, and M. M. Tentzeris, "A novel conformal RFID-enabled module utilizing ink-jet-printed antennas and carbon nanotubes for gas-detection applications," *IEEE Antennas Wireless Propag. Lett.*, vol. 8, pp. 653–656, Jan. 2009.
- [26] C. Occhiuzzi, C. Paggi, and G. Marrocco, "Passive RFID strain-sensor based on meander-line antennas," *IEEE Trans. Antennas Propag.*, vol. 59, no. 12, pp. 4836–4840, Dec. 2011.
- [27] B. S. Cook, J. Cooper, S. Kim, and M. M. Tentzeris, "A novel ink-jet-printed passive microfluidic RFID-based sensing platform," in *Proc. IEEE MTT-S Int. Microwave Symp.*, Seattle, WA, 2–7 June 2013.
- [28] J. Virtanen, L. Ukkonen, T. Bjorninen, A. Z. Elsherbeni, and L. Sydänheimo, "Ink-jet-printed humidity sensor for passive UHF RFID systems," *IEEE Trans. Instrum. Meas.*, vol. 60, no. 8, pp. 2768–2777, Aug. 2011.
- [29] R. Vyas, V. Lakafosis, H. Lee, G. Shaker, L. Yang, G. Orecchini, A. Traille, M. M. Tentzeris, and L. Roselli, "Ink-jet printed, self powered, wireless sensors for environmental, gas, and authentication-based sensing," *IEEE Sens. J.*, vol. 11, no. 12, pp. 3139–3152, Dec. 2011.
- [30] B. K. Park, D. Kim, S. Jeong, J. Moon, and J. S. Kim, "Direct writing of copper conductive patterns by ink-jet printing," *Thin Solid Films*, vol. 515, no. 19, pp. 7706–7711, July 2007.
- [31] S. B. Fuller, E. J. Wilhelm, and J. M. Jacobson, "Ink-jet printed nanoparticle microelectromechanical systems," *J. Microelectromech. Syst.*, vol. 11, no. 1, pp. 54–60, Feb 2002.
- [32] T. Le, V. Lakafosis, L. Ziyin, C. P. Wong, and M. M. Tentzeris, "Ink-jet-printed graphene-based wireless gas sensor modules," in *Proc. IEEE 62nd Electronic Components Technology Conf.*, May 29–June 1 2012, pp. 1003–1008.
- [33] Y. Nobusa, Y. Yomogida, S. Matsuzaki, K. Yanagi, H. Kataura, and T. Takenobu, "Ink-jet printing of single-walled carbon nanotube thinfilm transistors patterned by surface modification," *Appl. Phys. Lett.*, vol. 99, no. 18, pp. 183106–183106-3, Oct. 2011.
- [34] M. F. Mabrook, C. Pearson, and M. C. Petty, "Ink-jet-printed polymer films for the detection of organic vapors," *IEEE Sens. J.*, vol. 6, no. 6, pp. 1435–1444, Dec. 2006.
- [35] S.-Y. Han, D.-H. Lee, G. S. Herman, and C.-H. Chang, "Ink-jet-printed high mobility transparent-oxide semiconductors," *J. Display Technol.*, vol. 5, no. 12, pp. 520–524, Dec. 2009.
- [36] G. Shaker, S. Safavi-Naeini, N. Sangary, and M. M. Tentzeris, "Ink-jet printing of ultrawideband antennas on paper-based substrates," *IEEE Antennas Wireless Propag. Lett.*, vol. 10, no. 1, pp. 111–114, 2011.
- [37] J.-U. Park, M. Hardy, S. J. Kang, K. Barton, K. Adair, D. Mukhopadhyay, C. Y. Lee, M. S. Strano, A. G. Alleyne, J. G. Georgiadis, P. M. Ferreira, and J. A. Rogers, "High-resolution electrohydrodynamic jet printing," *Nature Mater.*, vol. 6, pp. 782–789, Aug. 2007.
- [38] B. S. Cook and A. Shamim, "Ink-jet printing of novel wideband and high gain antennas on low-cost paper substrate," *IEEE Trans. Antennas Propag.*, vol. 60, no. 9, pp. 4148–4156, 2012.
- [39] M. M. Tentzeris, R. Vyas, V. Lakafosis, T. Le, A. Rida, and S. Kim, "Conformal 2D/3D wireless modules utilizing ink-jet printing and nanotechnology," *Microwave J.*, vol. 33, no. 2, p. 20, Feb. 2012.
- [40] K. Maekawa, K. Yamasaki, T. Niizeki, M. Mita, Y. Matsuba, N. Terada, and H. Saito, "Drop-on-demand laser sintering with silver nanoparticles for electronics packaging," *IEEE Trans. Comp., Packag., Manufact. Technol.*, vol. 2, no. 5, pp. 868–877, 2012.
- [41] B. Polzinger, F. Schoen, V. Matic, J. Keck, H. Willeck, W. Eberhardt, and H. Kueck, "UV-sintering of ink-jet-printed conductive silver tracks," in *Proc. 2011 11th IEEE Conf. Nanotechnology*, 2011, pp. 201–204.
- [42] M. Allen, A. Alastalo, M. Suhonen, T. Mattila, J. Leppäniemi, and H. Seppä, "Contactless electrical sintering of silver nanoparticles on flexible substrates," *IEEE Trans. Microwave Theory Tech.*, vol. 59, no. 5, pp. 1419–1429, 2011.
- [43] J. Perelaer, A. W. M. de Laat, C. E. Hendriks, and U. S. Schubert, "Ink-jet-printed silver tracks: Low temperature curing and thermal stability investigation," *J. Mater. Chem.*, vol. 18, no. 27, pp. 3209–3215, 2008.
- [44] U. Caglar, K. Kaija, and P. Mansikkamäki, "Analysis of mechanical performance of silver ink-jet-printed structures," in *Proc. 2nd IEEE Int. Nanoelectronics Conf.*, 2008, pp. 851–856.
- [45] B. S. Cook, Y. Fang, S. Kim, T. Le, W. B. Goodwin, K. H. Sandhage, and M. M. Tentzeris, "Ink-jet catalyst printing and electroless copper deposition for low-cost patterned microwave passive devices on paper," in *Proc. Electronic Materials Letters*.
- [46] B. S. Cook, J. R. Cooper, and M. M. Tentzeris, "Multilayer RF capacitors on flexible substrates utilizing ink-jet-printed dielectric

- polymers," in *Proc. IEEE Microwave Wireless Components Letters*, to be published.
- [47] J. Riley, A. Smith, D. Reynolds, A. Edwards, J. Osborne, I. Williams, N. Carreck, and G. Poppy, "Tracking bees with harmonic radar," *Nature*, vol. 379, pp. 29–30, Jan. 1996.
- [48] G. Orecchini, V. Palazzari, A. Rida, F. Alimenti, M. Tentzeris, and L. Roselli, "Design and fabrication of ultra-low cost radio frequency identification antennas and tags exploiting paper substrates and ink-jet printing technology," *IET Microwave Antennas Propag.*, vol. 5, no. 8, pp. 993–1001, July 2011.
- [49] S. Helbing, M. Cryan, F. Alimenti, P. Mezzanotte, L. Roselli, and R. Sorrentino, "Design and verification of a novel crossed dipole structure for quasi-optical frequency doublers," *IEEE Microwave Guided Wave Lett.*, vol. 10, no. 3, pp. 105–107, Mar. 2000.
- [50] F. Alimenti and L. Roselli, "Theory of zero-power RFID sensors based on harmonic generation and orthogonally polarized antennas," *Prog. Electromagn. Res.*, vol. 134, pp. 337–357, Jan. 2013.
- [51] L. Yang, R. Zhang, D. Staiculescu, C. Wong, and M. Tentzeris, "A novel conformal rfid-enabled module utilizing ink-jet-printed antennas and carbon nanotubes for gas-detection applications," *IEEE Antennas Wireless Propag. Lett.*, vol. 8, pp. 653–656, Jan. 2009.
- [52] L. Yang, G. Orecchini, G. Shaker, H.-S. Lee, and M. Tentzeris, "Batteryfree RFID-enabled wireless sensors," in *IEEE MTT-S Int. Microwave Symp. Dig.*, May 2010, pp. 1528–1531.
- [53] R. Baccarelli, G. Orecchini, F. Alimenti, and L. Roselli, "Feasibility study of a fully organic, CNT based, harmonic RFID gas sensor," in *Proc. IEEE Int. Conf. RFID-Technologies Applications*, Nov. 2012, pp. 419–422.
- [54] S. Chopra, A. Pham, J. Gaillard, A. Parker, and A. Rao, "Carbon-nanotube-based resonant-circuit sensor for ammonia," *Appl. Phys. Lett.*, vol. 80, no. 24, pp. 4632–4634, June 2002.
- [55] R. Y. Miyamoto and T. Itoh, "Retrodirective arrays for wireless communications," *IEEE Microwave Mag.*, vol. 3, no. 1, pp. 71–79, Mar. 2002.
- [56] L. C. Van Atta, "Electromagnetic reflector," U. S. Patent 2 908 002, Oct. 1959.
- [57] A. M. Ali, H. B. El-Shaarawy, and H. Aubert, "Millimeter-wave substrate integrated waveguide passive Van Atta reflector array," *IEEE Trans. Antennas Propag.*, vol. 61, no. 3, pp. 1465–1470, Mar. 2013.
- [58] C. Y. Pon, "Retrodirective array using the heterodyne technique," *IEEE Trans. Antennas Propag.*, vol. AP-12, pp. 176–180, Mar. 1964.
- [59] C. W. Pobanz and T. Itoh, "A conformal retrodirective array for radar applications using a heterodyne phased scattering element," in *IEEE MTT-S Int. Microwave Symp. Dig.*, May 1995, vol. 2, pp. 905–908.
- [60] R. Y. Miyamoto, Y. Qian, and T. Itoh, "An active integrated retrodirective transponder for remote information retrieval-on-demand," *IEEE Trans. Microwave Theory Tech.*, vol. 49, no. 9, pp. 1658–1662, Sept. 2001.
- [61] P. Chan and V. Fusco, "Bi-static 5.8GHz RFID range enhancement using retrodirective techniques," in *Proc. 41st European Microwave Conf.*, 10–13 Oct. 2011, pp. 976–979.
- [62] Y.-J. Ren and K. Chang, "Bow-tie retrodirective rectenna," *Electron. Lett.*, vol. 42, no. 4, pp. 191–192, 16 Feb. 2006.
- [63] Y.-J. Ren and K. Chang, "New 5.8-GHz circularly polarized retrodirective rectenna arrays for wireless power transmission," *IEEE Trans. Microwave Theory Tech.*, vol. 54, no. 7, pp. 2970–2976, July 2006.
- [64] J. Cespedes, F. Giuppi, A. Collado, and A. Georgiadis, "A retrodirective UHF RFID tag on paper substrate," in *Proc. IEEE Int. Conf. RFID-Technologies Applications*, 5–7 Nov. 2012, pp. 263–266.
- [65] R. Bhattacharyya, C. Floerkemeier, and S. Sarma, "Low-cost, ubiquitous RFID-tag-antenna-based sensing," *Proc. IEEE*, vol. 98, no. 9, pp. 1593–1600, Sept. 2010.
- [66] S. Preradovic and N. C. Karmakar, "Chipless RFID: Bar code of the future," *IEEE Microwave Mag.*, vol. 11, no. 7, pp. 87–97, Dec. 2010.
- [67] S. Kim, B. Cook, J. Cooper, A. Traille, A. Georgiadis, H. Aubert, and M. Tentzeris, "Ink-jet-printed substrate integrated waveguide passive dual-band retro-directive array on paper substrate for chipless RFID tag and sensor applications," in *Proc. IEEE MTT-S Int. Microwave Symp.*, Seattle, WA, 2–7 June 2013, to be published.
- [68] M. Bozzi, A. Georgiadis, and K. Wu, "Review of substrate integrated waveguide circuits and antennas," *IET Microwaves, Antennas Propag.*, vol. 5, no. 8, pp. 909–920, June 2011.
- [69] R. J. M. Vullers, R. V. Schaijk, H. J. Visser, J. Penders, and C. V. Hoof, "Energy harvesting for autonomous wireless sensor networks," *IEEE Solid-State Circuits Mag.*, vol. 2, no. 2, pp. 29–38, Spring 2010.
- [70] M. Tanaka, R. Suzuki, Y. Suzuki, and K. Araki, "Microstrip antenna with solar cells for microsattellites," in *Proc. IEEE Int. Symp. Antennas Propagation*, 20–24 June 1994, vol. 2, pp. 786–789.
- [71] M. Danesh and J. R. Long, "An autonomous wireless sensor node incorporating a solar cell antenna for energy harvesting," *IEEE Trans. Microwave Theory Tech.*, vol. 59, no. 12, pp. 3546–3555, Dec. 2011.
- [72] T. Wu, L. RongLin, and M. M. Tentzeris, "A scalable solar antenna for autonomous integrated wireless sensor nodes," *IEEE Antennas Wireless Propag. Lett.*, vol. 10, pp. 510–513, Jan. 2011.
- [73] F. Declerq, A. Georgiadis, and H. Rogier, "Wearable aperture-coupled shorted solar-patch antenna for remote tracking and monitoring applications," in *Proc. 5th European Conf. Antennas Propagation*, Rome, Italy, 11–15 Apr. 2011, pp. 2992–2996.
- [74] A. Collado and A. Georgiadis, "Conformal hybrid solar and electromagnetic energy harvesting rectenna," *IEEE Trans. Circuits Syst. I*, to be published (early access IEEE Xplore DOI: 10.1109/TCSL.2013.2239154).
- [75] A. Georgiadis, A. Collado, S. Via, and C. Meneses, "Flexible hybrid solar/EM energy harvester for autonomous sensors," in *Proc. IEEE MTT-S Int. Microwave Symp.*, Baltimore, MD, 5–10 June 2011, pp. 1–4.
- [76] S. Kim, A. Georgiadis, A. Collado, and M. M. Tentzeris, "A ink-jet-printed solar-powered wireless beacon on paper for identification and wireless power transmission applications," *IEEE Trans. Microwave Theory Tech.*, vol. 60, no. 12, pp. 4178–4186, Dec. 2012.
- [77] A. P. Sample, J. Braun, A. Parks, and J. R. Smith, "Photovoltaic enhanced UHF RFID tag antennas for dual purpose energy harvesting," in *Proc. IEEE Int. Conf. RFID*, 12–14 Apr. 2011, pp. 146–153.
- [78] SL3S1203/1213 NXP's UCODE G2iL transponder IC. [Online]. Available: http://www.nxp.com/products/identification_and_security/smart_label_and_tag_ics/ucode/series/SL3S1203_1213.html
- [79] A. Georgiadis and A. Collado, "Improving range of passive RFID tags utilizing energy harvesting and high efficiency class-E oscillators," in *Proc. 6th European Conf. Antennas Propagation*, 26–30 Mar. 2012, pp. 3455–3458.
- [80] P. E. Glaser, "Power from the sun," *Science*, vol. 162, no. 3856, pp. 857–886, 1968.
- [81] J. O. McSpadden and J. C. Mankins, "Space solar power programs and microwave wireless power transmission technology," *IEEE Microwave Mag.*, vol. 3, no. 4, pp. 46–57, Dec. 2002.
- [82] H. Matsumoto, "Research on solar power satellites and microwave power transmission in Japan," *IEEE Microwave Mag.*, vol. 3, no. 4, pp. 36–45, 2002.
- [83] A. Georgiadis and A. Collado, "Solar powered class-E active antenna oscillator for wireless power transmission," in *Proc. IEEE Radio Wireless Week*, 20–23 Jan. 2013, pp. 40–42.

